

# Collective rheology in quasi static shear flow of granular media

Tamás Unger<sup>1,\*</sup>

<sup>1</sup>*HAS-BUTE Condensed Matter Research Group, Budapest  
University of Technology and Economics, H-1111 Budapest, Hungary*

This paper is devoted to the basic question of what factors determine the strain field in a quasi static granular flow. It is shown that using stress - strain rate relations is not the proper way to understand quasi static rheology. An alternative approach is discussed where the local deformation is regarded as the cause of deformation in the vicinity. We suggest a continuum model where the local shear strain is proportional to its Laplacian and the proportionality factor is determined by the local stress. The predicted behavior is tested in a three dimensional shear cell by means of computer simulations. The simplicity of our setup makes it ideal to demonstrate and examine the fundamental open questions of collective granular flows. The observed shear profile is interpreted in the framework of the suggested model.

## I. INTRODUCTION

When a granular material is deformed slowly in a simple plane shear cell [1–3] a critical state is reached after a transient period. This critical state is unique for the given granular material and is characterized e.g. by a well defined critical volume fraction  $\Phi_{\text{crit}}$  and a critical coefficient of effective friction  $\mu_{\text{crit}}$ . A nice property of the critical state is that it is devoid of memory effects in the sense that the preparation history does not play any role [2, 3]. The initial state of the contact network is destroyed and a self-organized inner fabric is maintained during the shear deformation.

The material constants  $\Phi_{\text{crit}}$  and  $\mu_{\text{crit}}$  are valid for quasi static shear of low inertia numbers  $I$  [1], i.e. when the shear rate is low enough and the pressure is large enough. In this paper we concentrate on the quasi static regime rather than on dense inertia flows. The dilute gas-like regime is out of scope of the present study.

The idea in the plane shear experiment is that the material is tested under uniform stress and strain conditions in order to deduce constitutive relations between local strain, strain rate and stress. Then with this knowledge one can try to understand the rheology in more complicated situations that often come up in applications. It is expected that a small homogeneous piece of bulk material of a large system behaves according to the plane shear experiment. One of the most interesting things about quasi static deformations is that the above concept does not work.

The meaning of the effective friction coefficient is the ratio of the shear stress measured in the shear direction divided by the perpendicular normal stress. What we learn from plane shear tests performed both in experiments and in computer simulations is that persistent shear flow needs a stress ratio at least  $\mu_{\text{crit}}$ . Once the imposed stress ratio drops below this threshold the flow stops and the material behaves as a solid body.

On the other hand if a bit more complicated setup is considered, e.g. a Couette cell [1], the above rule “solid-below-the-threshold” does not hold any more. The problem is more pronounced for split bottom shear cells [4–7] where wider shear zones and smoother flow profiles arise than in Couette flows. In these systems stationary shear flow is observed also in regions where the local stress ratio is far below the threshold  $\mu_{\text{crit}}$  [8, 9]. An extreme example is shown in [10] where sand behaves as a zero yield stress fluid, i.e. even a tiny shear stress is enough to cause deformation.

We conclude that such a collective flow can not be interpreted locally as a simple plane shear. Clearly, the local strain rate is not determined by the local stress tensor alone. What is then the underlying mechanism that determines the stress and strain fields? How does the material know locally how to deform? This is the basic mystery of quasi static shear flow that is in the focus of the present paper. To answer these questions is of fundamental importance in order to be able to predict rheology in various granular systems. Even a very simple geometry such as the straight split bottom cell [6, 8] represents a serious challenge for theories. We are not aware of any model in the granular literature that is able to provide the correct flow profile for this case. Let us refer to the above questions as the problem of collective rheology.

A popular approach to describe the flow is to assume the effective friction coefficient to depend on the local inertia parameter  $\mu_{\text{eff}}(I)$  and indeed it does a very good job for inertia flows [1, 11]. This technique fails, however, for quasi static flows. It can not describe the non-trivial smooth flow that emerges in the collective rheology and often predicts infinitely narrow shear bands instead [5, 12].

To study the problem of collective rheology it is a good start to deal with stationary flows for the sake of simplicity. Thus Couette or split bottom tests seem to be good choices. However, these systems are much more complicated than the plane shear experiment, they involve too many degrees of freedom and unnecessary difficulties. Just to mention one, the material layers that slide next to each other during the flow are curved in one way

---

\*Electronic address: unger@phy.bme.hu

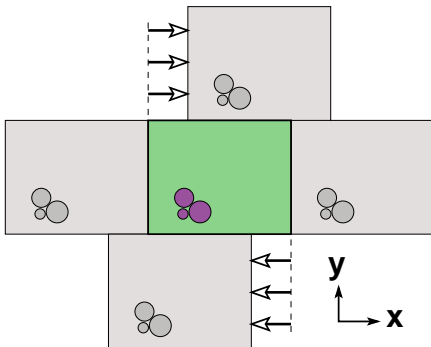


FIG. 1: Schematic illustration of the shear cell used in the computer simulations. The shear cell is three dimensional where Lees-Edwards boundary condition is applied in  $y$  direction while in  $x$  and  $z$  directions normal periodic boundaries are used.

or another, which affects the stress field in a non-trivial way [6] and makes the treatment harder. To shed more light on the mystery it is better to start with the simplest possible system where the problem of collective rheology arises. In this article we suggest and analyze such a test system, which is only one step away from the homogeneous plane shear.

The shear flows investigated here are achieved inside the computer by means of discrete element simulations. We deal with three dimensional flows of frictional and spherical grains. The paper is structured as follows. First we examine the important reference situation of the quasi static critical state produced in homogeneous plane shear. Then we modify the system to achieve non-trivial collective flow and present the results of the simulations. In the last part we suggest a model that can account for some of the features of this collective behavior.

## II. HOMOGENEOUS PLANE SHEAR

### A. The influence of the inertia parameter

The computer simulations are carried out by the algorithm of contact dynamics (CD) [13–16]. The dynamics, as usual, is governed by Newton’s equation of motion applied for each grain. The interaction of the grains are handled by means of constraint forces at the contact points which are determined based on the assumption that the grains are rigid (undeformable).

Our shear cell uses Lees-Edwards boundary condition in order to attain homogeneous plane shear (see Fig. 1). That is the system is periodically connected in  $y$  direction in a special way: There is a velocity difference  $v_{\text{shear}}$  between the upper and lower boundary which provides the shearing. In  $x$  and  $z$  directions normal periodic boundaries are used. Thus confining walls are completely avoided and shearing is achieved by the special periodic boundaries alone. This is advantageous because walls

would introduce undesired boundary effects (e.g. layering) that significantly can alter the behavior especially of small systems used in computer simulations. This way the system is a priori translational invariant in  $x$ ,  $y$  and  $z$  directions, there are no special points, everywhere is “inside the bulk”. The pressure conditions are controlled by Andersen boundary conditions [17], i.e. by properly varying the volume. Details how this is implemented in CD can be found in [15]. In all the simulations gravity is set to zero.

Thus our system is sheared in the  $xy$  plane in  $x$  direction and the two following parameters are kept constant during the simulation: the global shear rate  $\dot{\gamma} = v_{\text{shear}}/(2L_y)$ , where  $L_y$  is the system size in  $y$  direction, and the  $yy$  component of the stress tensor ( $\sigma_{yy}$ ). All simulations presented in this paper are performed with the help of the above shear cell.

In the first set of simulations we examine one system in various conditions. This test system consists of 2500 spherical grains with radii distributed uniformly between the unit length 1.0 and 1.3. The friction coefficient  $\mu_{\text{cont}}$  of the grain-grain contacts is set to 0.2 (for both static and dynamic friction). We are interested in the steady state properties therefore relatively large shear displacement is simulated for each run. The value of the total shear strain  $\gamma = \Delta l_{\text{shear}}/(2L_y)$  (given by half of the total shear displacement in  $x$  direction divided by the system size in  $y$  direction) is typically of the order of 100. Even for the smallest inertia number where the simulation is very computation consuming  $\gamma$  is chosen larger than 20.

We examine whether the inertia parameter  $I$  [1] serves as a good control parameter that determines the state of the system. The inertia parameter is defined as

$$I = \dot{\gamma} d \sqrt{\rho/p}, \quad (1)$$

where  $d$ ,  $\rho$  and  $p$  are the typical grain size, the mass density of grains and the pressure, respectively. The inertia parameter reflects the scale of the inertia forces with respect to the force scale generated by the pressure. Low inertia parameter means that the inertia forces that cause accelerations of the grains are much smaller than the typical contact forces between the grains. The definition of  $p$  is ambiguous because the stress tensor is not spherical. Here we use  $\sigma_{yy}$  in place of  $p$ , however, this choice is unimportant in the scope of the present study. Using any of the normal stress components or  $\text{Tr}(\sigma)/3$  would lead to negligible change in the value of  $I$ .

We focus basically on two indicators of the state of the material, the density and the resistance against shear. More precisely, these are the solid fraction  $\Phi$  which gives the total solid volume of the grains divided by the volume of the system and the effective friction  $\mu_{\text{eff}}$  provided by the ratio of two elements of the stress tensor  $\sigma_{xy}/\sigma_{yy}$ . We measure the time averaged  $\Phi$  and  $\mu_{\text{eff}}$  in the stationary flow and plot these data as the function of the inertia parameter.

In Fig. 2 the results for the solid fraction are shown. We scanned through a wide region of  $I$  by systematically

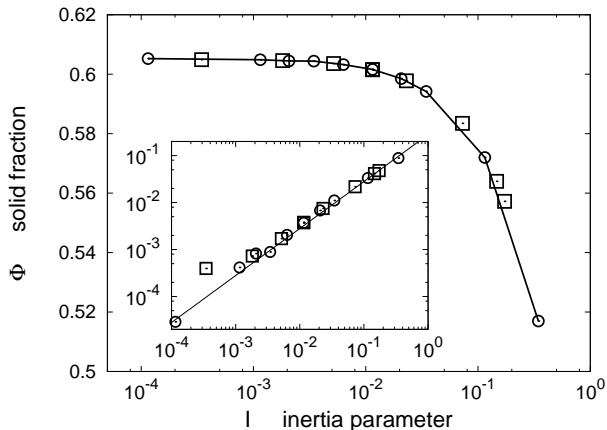


FIG. 2: The solid fraction  $\Phi$  is plotted against the inertia parameter  $I$ . The circles connected by the solid line show a set of simulations which differ only in the driving shear rate  $\gamma$ , while squares stand for simulations where other parameters are also varied in a random manner such as the mass density of grains, the pressure and the technical parameter  $\Delta t$  which is the time step of the algorithm. The inset shows the difference from the critical value ( $\Phi_{\text{crit}} - \Phi(I)$ ) against  $I$  in log-log scale. The straight line indicates slope 1.

changing the driving shear rate  $\gamma$ , while keeping all other input parameters fixed. Other simulations were also performed where we tested several random combinations of the input parameters: The pressure and mass density of the grains were changed by factors over 1000, the time step used by the simulation code was also varied by a factor 50. It can be seen that putting all these data in one plot make them collapse on a single curve. The influence of other physical and technical parameters (not shown here) were also tested: The size of the system [20], the inertia used by the Andersen type of pressure control and the number of force-iterations [14] used by the contact dynamics algorithm are all parameters that within a wide range have no effect on the value of  $\Phi$ .

Thus we conclude that in case of our virtual material the inertia number  $I$  is indeed the key control parameter and it determines the solid fraction uniquely in homogeneous plane shear. Exactly the same holds for the effective friction  $\mu_{\text{eff}}$  and other ratios of the elements of the stress tensor which are also unique functions of  $I$  as shown in Fig. 3 and Fig. 4.

In Figs. 2, 3 and 4, where the  $I$  axis is in logarithmic scale, all the plotted quantities reach a plateau for small inertia numbers. This plateau region can be regarded approximately as the quasi static region. Its upper bound, i.e. the largest quasi static value of  $I$ , depends on the required accuracy. The ideal quasi static flow is, in fact, a mathematical limit case of  $I \rightarrow 0$ . The homogeneous and stationary plane shear in the quasi static limit can be characterized by the well defined critical values:

$$\mu_{\text{crit}} = \lim_{I \rightarrow 0} \mu_{\text{eff}}(I) \quad \text{and} \quad \Phi_{\text{crit}} = \lim_{I \rightarrow 0} \Phi(I). \quad (2)$$

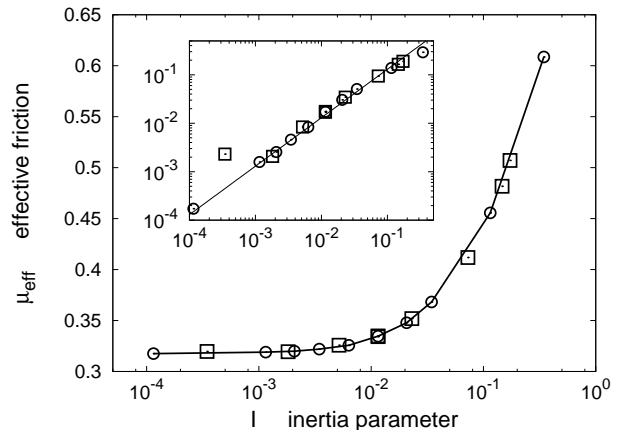


FIG. 3: The effective friction  $\mu_{\text{eff}}$  is plotted against the inertia parameter  $I$ . The symbols (circles and squares) have the same meaning as in Fig. 2. The inset shows the deviation from the critical value ( $\mu_{\text{eff}}(I) - \mu_{\text{crit}}$ ) against  $I$  in log-log scale. The straight line indicates slope 1.

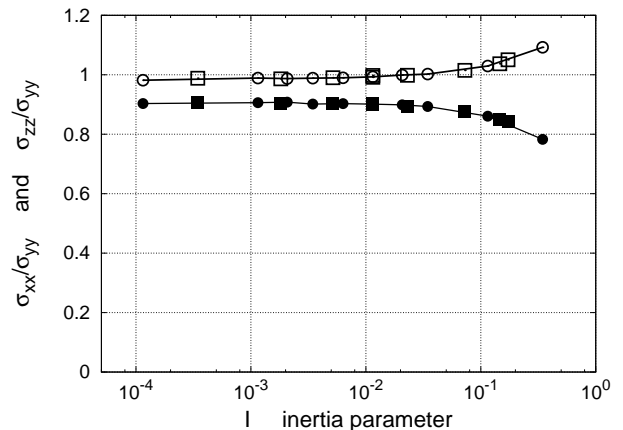


FIG. 4: The ratios of normal stresses are shown as the functions of the inertia parameter  $I$ . Open and closed symbols stand for  $\sigma_{xx}/\sigma_{yy}$  and  $\sigma_{zz}/\sigma_{yy}$ , respectively. Circles and squares have the same meaning as in Fig. 2.

In our simulations we find that the deviations of  $\Phi$  and  $\mu_{\text{eff}}$  from the corresponding critical values are proportional to  $I$  for small inertia numbers (insets in Figs. 2, 3).

An interesting feature of the normal stresses is shown in Fig. 4. Regarding the  $xy$  shear plane the values of normal stresses  $\sigma_{xx}$  and  $\sigma_{yy}$  are very close to each other provided the system is sheared quasi statically. In perpendicular direction, however, the normal stress  $\sigma_{zz}$  turns out to be lower about 10 percent. This weak stress response in side direction might be an important factor in real three dimensional flows and lead to a non-trivial stress distribution throughout the system.

In this section we examined how the quasi static critical state (in short critical state) can be approximated by low inertia numbers. The simulations presented in

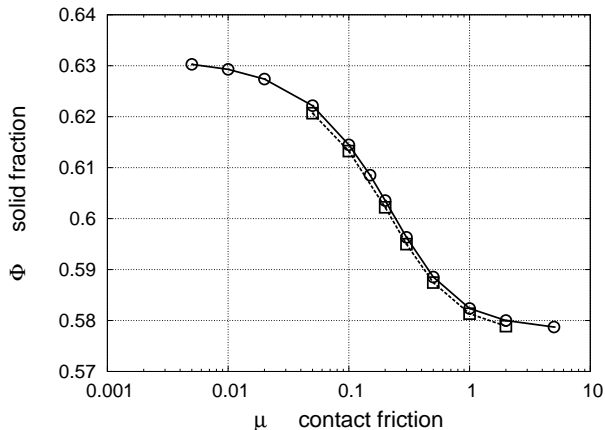


FIG. 5: The solid fraction  $\Phi$  is plotted against the friction coefficient of the grain-grain contacts. The data shown by circles and squares are obtained in polydisperse and monodisperse systems, respectively.

the rest of the paper remain as near as possible to this ideal quasi static limit. This effort is bounded by the available computational capacity because lower inertia numbers require more calculations.

### B. The effect of contact friction and size distribution on the critical state

In this section we study how the critical state differs for different materials. The materials used in our simulations differ either in the coefficient of contact friction  $\mu$  or in the size distribution of the spherical grains. We use either a polydisperse system similarly to the previous section, i.e. with grain radii chosen uniformly between 1.0 and 1.3, or a monodisperse system with grain radius 1.0. The inertia parameters are set to  $5.2 \times 10^{-3}$  and  $4.5 \times 10^{-3}$  for polydisperse and monodisperse simulations, respectively. The systems consist of 5000 grains each and are tested with various values of  $\mu$ . The properties of the critical state are measured and averaged over a typical total shear strain  $\gamma \approx 30$ .

In Fig. 5, 6 and 7 we show the behavior of the quantities  $\Phi$ ,  $\mu_{\text{eff}}$  and the normal stress ratios. Because the applied inertia parameters are relatively low, these measured values can be regarded as approximate critical values. Actually, the deviations between the data shown here and the exact critical values can be estimated based on the results of the previous section. For example the exact curve  $\mu_{\text{crit}}(\mu)$  is expected to be slightly lower than the values of  $\mu_{\text{eff}}$  shown in Fig. 6 and the estimated deviation is only around  $6 \times 10^{-3}$ .

It is astonishing how little difference the polydispersity makes. It would clearly be a different situation if we had much larger fluctuations in the grain sizes. However, the level of polydispersity examined here has basically no impact compared to a system of identical beads neither

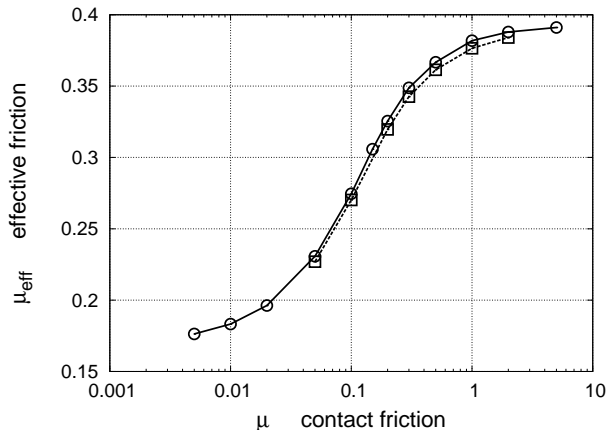


FIG. 6: The effective friction  $\mu_{\text{eff}}$  is plotted against the friction coefficient of the grain-grain contacts. The data shown by circles and squares are obtained in polydisperse and monodisperse systems, respectively.

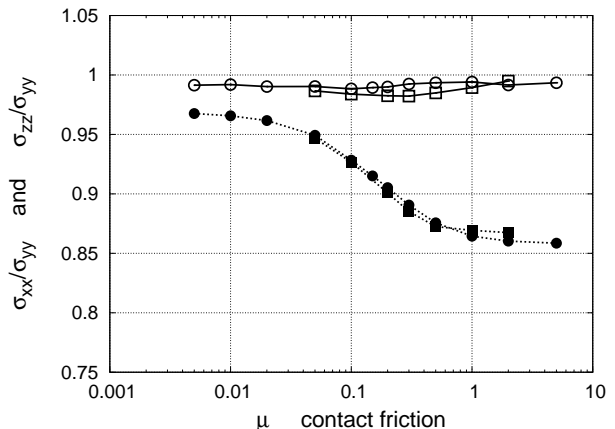


FIG. 7: The ratios of normal stresses are plotted against the friction coefficient of the grain-grain contacts. Open symbols show  $\sigma_{xx}/\sigma_{yy}$  while closed symbols denote  $\sigma_{zz}/\sigma_{yy}$ . The data distinguished by circles and squares are obtained in polydisperse and monodisperse systems, respectively.

on the density nor on the stress tensor.

The critical state, on the other hand, is very sensitive to the inter-particle friction coefficient  $\mu$ . For example when changing  $\mu$  the critical solid fraction (Fig. 5) explores almost the whole range between the two limits  $\Phi_{\text{RLP}}$  and  $\Phi_{\text{RCP}}$  that are commonly attributed to the random loose and random close packings.

The fact that the effective friction depends strongly on  $\mu$  is important in the present scope. This property will be exploited later to study the problem of the collective rheology.

We find (Fig. 7) that the normal stresses in the shear plane ( $\sigma_{xx}$  and  $\sigma_{yy}$ ) remain approximately equal for the whole range of  $\mu$  as we saw this for one particular case in section II A. Also the normal stress in side direction  $\sigma_{zz}$  appears to be weaker than the other two. However, the



friction  $\mu$  has a significant influence on this weakening effect: While for large  $\mu$  the weakening is about 14 percent, it drops down to 3 percent with vanishing friction coefficient.

### III. BEYOND THE HOMOGENEOUS CASE

#### A. The shear profile

So far we focused on the homogeneous plane shear and examined the properties of the critical state. In this section we turn to the case of an inhomogeneous shear flow that is still relatively simple, stationary and quasi static. We show that the behavior can not be interpreted based on the critical state of the material.

When our shear cell is filled with one material as in the previous section, the flow is indeed homogeneous. We find e.g. that the local stress tensor averaged over time is the same everywhere in the shear cell. The time averaged local velocity of the flow is parallel to the  $x$  axis and the speed is proportional to the  $y$  coordinate. Thus the local shear rate is independent of the position.

The inhomogeneity is introduced into the flow by using two different materials. The upper half of the shear cell ( $y > L_y/2$ ) is filled with grains of contact friction  $\mu_{\text{up}}$  that is chosen to be larger than the value  $\mu_{\text{lo}}$  that is used in the lower half ( $y < L_y/2$ ). We recall that there is no gravity in the simulation, “up” refers only to the orientation of the  $y$  axis. Apart from the coefficient of the contact friction there is no difference between the two materials.

The main question is how the shear strain is distributed throughout the system. The shear cell still remained translation invariant in  $x$  and  $z$  directions and no local property is expected to depend on these coordinates. We will focus on the  $y$  dependence of the measured quantities, especially of the local shear strain. For such measurements the system is divided into thin layers of thickness  $\Delta y$  parallel to the  $xz$  plane. When the value of a measured quantity is reported later as the function of  $y$  it means that it is calculated for each layer, averaged over  $x$ ,  $z$  and time over the whole range and over  $y$  within the given layer.

To set up and study the above suggested system (or an equivalent one) in real experiments might be very difficult. However, this shear cell suits well to computer simulations and is very instructive regarding the problem of collective rheology. As mentioned before, our goal is to avoid unnecessary complications and study the simplest possible system where the problem can be observed. The advantage of our system over traditional shear cells (like Couette cell, cylindrical and straight split bottom cells) is manifold: (i) the layers that slide next to each other in the shear flow are not curved but are straight planes [6], still stationary flow can be maintained. (ii) Due to the high degree of symmetry local quantities are not multivariate functions. They depend only on one parameter,

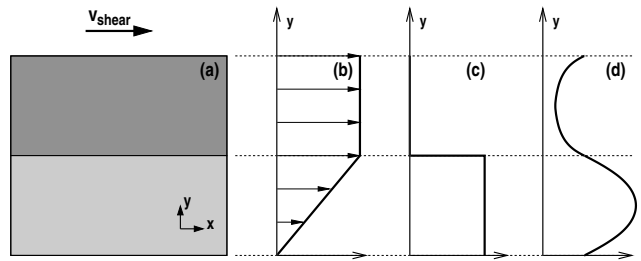


FIG. 8: (a) Sketch of the shear cell. The material in the upper part has larger coefficient of contact friction than that in the lower part. (b) and (c) The velocity  $v(y)$  and the corresponding shear strain is shown, respectively, that are suggested by the relation  $\mu_{\text{eff}}(I)$  obtained for homogeneous plane shear. (d) For comparison, the shear strain is drawn qualitatively that is observed in the computer simulations.

the coordinate  $y$ . (iii) Due to mechanical equilibrium the local shear stress  $\sigma_{xy}$  and the normal stress  $\sigma_{yy}$  are bound to be constant (do not depend on  $y$ ). Thus the spatial stress distribution is a priori very simple.

How does such a system deform? What we could naively expect based on the results of the homogeneous case is the following. Let us consider the lower material first which is easier to shear. As  $\sigma_{xy}/\sigma_{yy}$  does not depend on  $y$  the apparent effective friction is constant throughout the lower material and so is the local inertia parameter (Fig. 3). This gives a constant shear rate  $\dot{\gamma}(y)$  and a linear velocity profile in this region (Fig. 8). As the inertia parameter is kept very small the stress ratio  $\sigma_{xy}/\sigma_{yy}$  must be close to the plateau value of the effective friction of the lower material  $\mu_{\text{crit,lo}}$ . The same stress ratio must be valid also in the upper part of the system. However, this stress ratio is not enough to cause shear deformation at any rate in the upper material because here the contact friction and therefore also the critical value  $\mu_{\text{crit,up}}$  is higher than in the lower material (Fig. 6). Thus the overall stress ratio  $\sigma_{xy}/\sigma_{yy}$  is smaller than the minimum value ( $\mu_{\text{crit,up}}$ ) that would be needed to maintain shear flow. This naive argument leads us to the conclusion that the upper material does not deform at all. The local shear rate  $\dot{\gamma}(y)$  is constant in the lower part and zero in the upper one.

This is in contrast to our numerical measurement where different behavior is found (Fig. 8d). The observed flow does not support the assumption that there is a one to one relation between the local effective friction and the local inertia parameter. The function  $\mu_{\text{eff}}(I)$  that has been found in the homogeneous case is clearly not valid here.

Regarding the inhomogeneous case, we present three computer simulations *A*, *B* and *C* and the parameters of the simulations are as follows. The systems are monodisperse (every grain radius is 1.0), include 5000 grains each, and are subjected to a typical global shear strain  $\gamma_{\text{glob}} = \Delta l_{\text{shear}}/(2L_y) \approx 100$ . The driving shear rate  $\dot{\gamma}_{\text{glob}}$  and the vertical pressure  $\sigma_{yy}$ , which are kept constant in

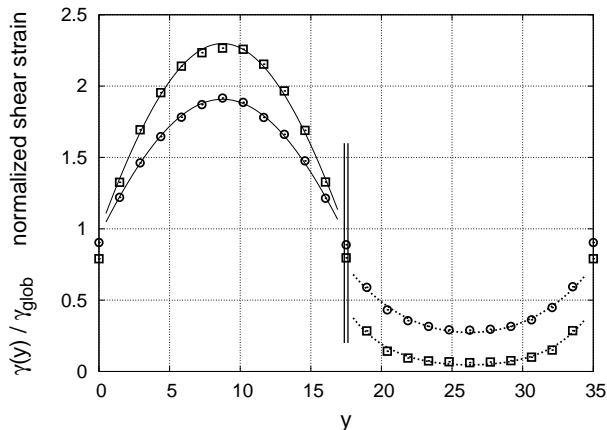


FIG. 9: The normalized shear strain is shown for systems *A* (circles) and *C* (squares) as the function of the vertical position  $y$ . Both systems have the same position of the interface indicated by the double vertical line. The pair of contact frictions  $(\mu_{lo}, \mu_{up})$  used below and above the interface is  $(0.1, 0.2)$  for *A* and  $(0.1, 0.5)$  for *C*. The data are fitted by cosine (hyperbolic cosine) functions shown by the solid (dotted) lines.

time, are chosen to be quasi static: The corresponding global inertia parameter  $I_{glob}$  is  $5 * 10^{-4}$  in each case. In system *A* and *B* the pair of contact frictions  $(\mu_{lo}, \mu_{up})$  is set to  $(0.1, 0.2)$  while for system *C* the contrast is larger:  $(0.1, 0.5)$ . In case of *A* and *C* the two materials occupy half and half of the shear cell as described before. This is different for system *B* where the  $y$ -position of the interface is set to  $0.7 L_y$  thus the width of the region of small (large) friction is 70 (30) percent of the width  $L_y$  of the shear cell.

During the shear flow grains of the two materials could, in principle, diffuse and mix. This effect is not in the present focus, however, in the long run (in the time scale of mixing) would significantly alter the shear profile. To avoid this interference we exploit the possibility provided by the computer simulation and switch off the mixing effect as follows. If a grain-grain contact is located below or above the interface then its friction coefficient is set to  $\mu_{lo}$  and  $\mu_{up}$ , respectively. Thus contact friction is a property of the position and not of the grains in these simulations which results in a sharp interface between the two materials during the flow. In real experiments mixing can not be avoided in this way. We note, however, that due to separation of time scales such interfaces can exist long enough and mixing does not necessarily become an issue [18, 19].

The data on the observed shear profiles are shown in Figs. 9 and 10 where the local shear strain is plotted divided by the global shear strain that was applied to the shear cell  $(\gamma(y)/\gamma_{glob})$ . These data are equivalent to the normalized shear rate  $\dot{\gamma}(y)/\dot{\gamma}_{glob}$  and as long as the flow is quasi-static the observed curves are independent of the driving shear rate  $\dot{\gamma}_{glob}$ . In each system the steady state involves shear deformation of both the lower and the

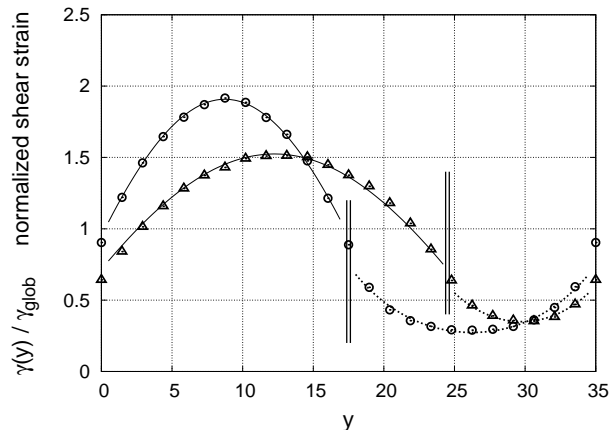


FIG. 10: The normalized shear strain is shown for systems *A* (circles) and *B* (squares) as the function of the vertical position  $y$ . Both systems have the same pair of contact frictions  $(\mu_{lo}, \mu_{up})$  used below and above the interface:  $(0.1, 0.2)$ . They differ only in the position of the interface as indicated by the double vertical lines. The data are fitted by cosine (hyperbolic cosine) functions shown by the solid (dotted) lines.

upper materials. These simulations demonstrate clearly that various values of the local shear rate are possible for the same local stress. The measured effective friction  $\mu_{eff} = \sigma_{xy}/\sigma_{yy}$ , which can be interpreted as the shear resistance that the inhomogeneous system collectively develops against the external driving, turns out to be very similar in all cases *A*, *B* and *C*:  $\mu_{eff} = 0.275 \pm 0.003$ . This value is somewhat larger than the estimated critical friction for the lower material:  $\mu_{crit}(\mu = 0.1) \approx 0.264$  and smaller than those for the two high-friction materials:  $\mu_{crit}(\mu = 0.2) \approx 0.314$  and  $\mu_{crit}(\mu = 0.5) \approx 0.356$ .

## B. Tentative description

How can we interpret the behavior presented in Figs. 9 and 10? Why does, in the first place, the region of  $\mu_{up}$  flow at all for shear stresses that are too weak to maintain flow in the homogeneous case? Presumably, the material of  $\mu_{up}$  remains solid for such stresses only if there is no flow around. However the same material can not retain the same static shear stress in the inhomogeneous situation because the lower part of the system flows already. This flow provides a kind of noise in the force network of the upper material. Thus the region that is expected to be solid is exposed to permanent agitation which must be quite strong near the interface. Under these noisy conditions the inner fabric might fail from time to time which results in a creep motion in the direction of the local shear stress no matter how weak this shear stress is. The key concept must be in our view that local deformation represents also the source of agitation [10]. Even without knowing exactly the nature of the agitation effect it seems to be plausible that this mechanism is responsible for the

observed quasi static rheology in various systems. The agitations arising from the nearby flow was expected to rule out static shear stresses also in the experiment [10] where sand was turned into a zero yield stress fluid.

Let us set up a tentative model in the spirit of the above picture to describe the rheology seen in the previous section. We consider an array of narrow parallel layers perpendicular to the  $y$  axis with their width  $\xi$  much smaller than the system size. The shear strain of the  $i$ th layer is denoted by  $\gamma_i$ . The value  $\sigma_{yy}$ , which is a fixed constant in the simulation, is taken as the unit of stress and we express the shear stress in this unit  $\tau = \sigma_{xy}/\sigma_{yy}$ . We assume about the local shear strain  $\gamma_i$  that it depends on two factors, on the local shear stress and on the amount of agitation that the  $i$ th layer receives. Furthermore, the deformation of the neighboring layers serves as the source of agitation, i.e. the amount of agitation received by the layer  $i$  is the function of  $\gamma_{i-1}$  and  $\gamma_{i+1}$  only. We put this in the following form:

$$\gamma_i = (\gamma_{i-1} + \gamma_{i+1})f(\tau), \quad (3)$$

where the plausible assumption is taken that the caused deformation  $\gamma_i$  is proportional to the deformation  $\gamma_{i-1} + \gamma_{i+1}$  that creates it. About the effect of  $\tau$  we assume only that it is given by a monotonous increasing function  $f(\tau)$  that may be different for different materials. It means that for the same amount of agitation the resulting strain grows with the shear stress. Eq. 3 is equivalent to the discrete equation:

$$\frac{\gamma_{i-1} + \gamma_{i+1} - 2\gamma_i}{\xi^2} = \frac{2}{\xi^2} \left[ \frac{1}{2f(\tau)} - 1 \right] \gamma_i. \quad (4)$$

In a continuum description (on length scales larger than  $\xi$ ) this corresponds to the following differential equation for  $\gamma(y)$ :

$$\frac{\partial^2 \gamma}{\partial y^2} = C(\tau)\gamma, \quad (5)$$

where  $C(\tau)$  is a material dependent function of the shear stress

$$C(\tau) = \frac{2}{\xi^2} \left[ \frac{1}{2f(\tau)} - 1 \right]. \quad (6)$$

The aim of Eq. 5 is to apprehend the shear profile in the studied flow which is quasi static and stationary. The structural form of the equation seems to be appropriate: it does not involve time and time derivatives which is a nice feature for a quasi static model, furthermore, if  $\gamma(y)$  is a solution then  $\lambda\gamma(y)$  is a solution as well for any number  $\lambda$  as it should be in steady state.

Let us consider the homogeneous situation first where  $\gamma(y)$  is independent of  $y$  and  $\tau$  is equal to the critical stress ratio  $\tau_{\text{crit}}$ . Then the left hand side of Eq. 5 is zero and the value of  $C(\tau)$  must vanish for  $\tau_{\text{crit}}$ . It also gives  $f(\tau_{\text{crit}}) = 1/2$ . This has an important consequence beyond the homogeneous case, namely, that the sign of

$C$  is different below and above the critical shear stress. Because  $f(\tau)$  is monotonous increasing:

$$\begin{aligned} C(\tau) > 0 & \quad \text{if } \tau < \tau_{\text{crit}}, \\ C(\tau) < 0 & \quad \text{if } \tau > \tau_{\text{crit}}. \end{aligned} \quad (7)$$

Eq. 5 allows quasi static flow also for shear stresses below and above the critical value  $\tau_{\text{crit}}$  and it makes also possible that different parts of the material exhibit different extent of deformation under the same local stress. This is in contrast to the naive picture we deduced alone from the homogeneous simulations of section II A.

The shear resistance that the material sets up against the external driving may be smaller or also larger than the critical value seen in the homogeneous plane shear. Thus not only softening but also hardening is possible compared to this reference state. Eq. 5 tells us that the deviation from the critical stress results in a curved shear profile  $\gamma(y)$ . The curvature is positive (negative) for smaller (larger) values of  $\tau$ .

$\tau$  is constant in space in our shear cell for both the homogeneous and the inhomogeneous simulations. Therefore  $C(\tau)$  is always a constant throughout one material and for such a region the functional form of  $\gamma(y)$  can be easily determined from Eq. 5.

$$\gamma_{\text{lo}}(y) = A_{\text{lo}} \cos[k_{\text{lo}}(y - y_c)] \quad (8)$$

for the lower materials in Figs. 9 and 10 where  $y_c$  is the actual middle position of the given region (where we utilized the mirror symmetry of the setup with respect to the symmetry plane of position  $y_c$ ). The parameter  $k_{\text{lo}}$  is given by  $C_{\text{lo}}(\tau) = -k_{\text{lo}}^2$ , where  $C$  is indeed negative as  $\tau > \tau_{\text{crit}}$  and the curvature of  $\gamma$  is also negative. For the upper materials where in each case the overall shear stress  $\tau$  is smaller than  $\tau_{\text{crit}}$  of the given material the value  $C_{\text{up}}(\tau)$  is positive and the corresponding solution has positive curvature:

$$\gamma_{\text{up}}(y) = A_{\text{up}} \cosh[k_{\text{up}}(y - y_c)], \quad (9)$$

where  $k_{\text{up}}^2 = C_{\text{up}}(\tau)$ .

The above model gives nice interpretation of some features of the quasi static behavior. As mentioned already both softening and hardening is possible. Hardening is interpreted that the  $i$ th layer gets less amount of agitation per unit shear strain than it needs for homogeneous deformation. The reduced level of agitation is connected to negative curvature of the shear profile  $\gamma(y)$  and makes the material harder to shear ( $\tau > \tau_{\text{crit}}$ ). Softening compared to the reference critical state is the opposite case which involves enlarged level of agitations, positive curvature of  $\gamma$  and smaller shear stress than the critical one. The model also does a good job in predicting the functional form of the shear profile as the functions cosine and hyperbolic cosine match the observed data of  $\gamma(y)$  very well (Figs. 9 and 10).

There are of course many questions left open in our quasi one dimensional shear cell which are important also

to understand quasi static flows in general. For example we can not calculate the parameters  $k_{lo}$  and  $k_{up}$  as we do not know the function  $C(\tau)$ . The prediction of ratio  $A_{lo}/A_{up}$  is also missing here. Therefore all these quantities are fit parameters in Figs. 9 and 10. The predicted curves are fitted only inside the given material, data points at the boundaries are not included because they represent an average shear strain in the vicinity of the interface involving both materials.

In the above picture the shear stress  $\tau$  determines  $k$  but not the amplitude. In the lower material  $A_{lo}$  depends only on the amount of agitation that this region gets through the boundaries, that is, on the agitation that is generated by the other material and transmitted through the two interfaces. In turn,  $A_{up}$  is determined by the transmitted agitation through the interfaces in the other direction towards the upper material. There is no reason why  $\gamma(y)$  should be continuous at such material interfaces. At this point we are not able to tell the boundary condition for  $\gamma(y)$  since not enough is known about the agitation mechanism.

### C. The solid fraction

Let us consider the inhomogeneous shear flow in our shear cell and the local state of the material at a given  $y$  position. How does this state differ from the critical state of the same material obtained in the homogeneous case? We argued that the two situations are somehow different in two quantities, in the amount of the hypothetical agitation per unit shear strain and in the more specific stress ratio  $\sigma_{xy}/\sigma_{yy}$  under which the flow occurs. Here we would like to emphasize and demonstrate it more clearly that the two states are different, even in the inner structure of the material.

This can be well seen if we plot the local solid fraction  $\Phi(y)$  measured in the inhomogeneous flow. Fig. 11 shows the data for simulation *A*, where also the critical solid fractions of the two materials are shown for comparison that were obtained by homogeneous plane shear. The lower material exhibit a solid fraction in this stationary and quasi static flow that is smaller than its well defined critical value. The upper material does the opposite, it gets denser compared to its critical density. We interpret the phenomenon as follows. The shear deformation tends to create pores between the grains while agitations, a sort of random shaking, tends to destroy these pores and drive the material towards a relatively dense structure. Compared to the homogeneous situation the upper material is deformed in an environment with increased level of agitation therefore the densification works better. For the lower material the reduced level of agitation results in looser structure than in the critical state.

Whether the speculation about the agitation level is right or not, the effect is clearly shown that the lower material is packed looser than in its critical state while the upper material gets denser than its own critical den-

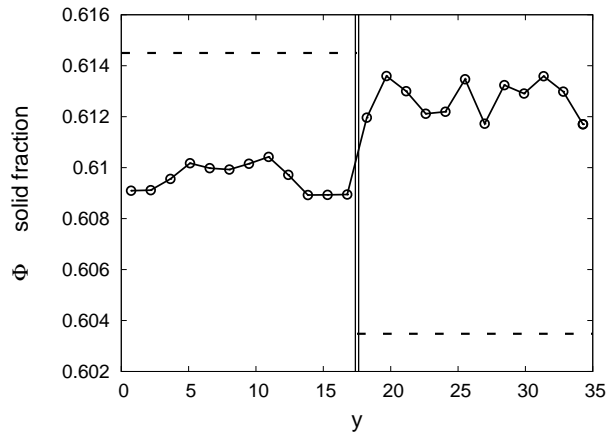


FIG. 11: The local solid fraction is plotted for simulation *A* as the function of the vertical position  $y$ . The double vertical line indicates the position of the interface between the lower and the upper materials. For both materials the horizontal dashed lines show the values  $\Phi_{crit}$ , i.e. the corresponding solid fractions in case of a quasi static homogeneous plane shear.

sity. This effect is so strong that actually the order of the densities of the two materials is reversed. This is surprising because it is expected that spherical grains with larger contact friction have lower solid fraction. Here we find the opposite within one system in a stationary flow.

## IV. SUMMARY

This paper is subjected to the quasi static flow of granular materials. We argued that quasi static rheology is a collective phenomenon that can not be interpreted locally as a simple plane shear. In general, the collective flow can exhibit such local states of the material that do not exist at all in homogeneous plane shear tests. Therefore it is difficult to isolate these states and study them separately. Even if we restrict the study to quasi static and stationary shear flows the physical properties of a mesoscopic piece of bulk material can be very different from the properties of the well defined critical state (e.g. density, shear resistance). The collective rheology can not be understood merely based on a constitutive relation that connects the local stress to the local strain and strain rate.

We analyzed a rather simple shear cell that was designed to demonstrate these fundamental problems of collective granular flows. We used three dimensional computer simulations and analyzed the spatial distribution of the stress and strain. We discussed a physical picture that may help to understand the observed flow in which the local deformation agitates the surrounding material and therefore creates deformation. We set up a tentative continuum model that essentially states that the local shear strain  $\gamma$  is proportional to its Laplacian  $\Delta\gamma$  and the factor between them is determined by the local



stress. The shear profile predicted by the model is in nice agreement to the observed deformation in our quasi one dimensional system.

### Acknowledgments

The author acknowledges support by the Bolyai János research program and by the Hungarian Scientific Re-

search Fund (grant No. PD073172).

- 
- [1] GDR\_MiDi, Eur. Phys. J. E **14**, 341 (2004).
  - [2] R. F. Craig, *Craig's soil mechanics* (Spon Press, New York, 2004).
  - [3] F. Radjai and S. Roux, in *The Physics of Granular Media* (Wiley-VCH, Weinheim, 2004), pp. 165–187.
  - [4] D. Fenistein, J. W. van de Meent, and M. van Hecke, Phys. Rev. Lett. **92**, 094301 (2004).
  - [5] T. Unger, J. Török, J. Kertész, and D. E. Wolf, Phys. Rev. Lett. **92**, 214301 (2004), cond-mat/0401143.
  - [6] M. Depken, W. van Saarloos, and M. van Hecke, Phys. Rev. E **73**, 031302 (2006).
  - [7] X. Cheng, J. B. Lechman, A. Fernandez-Barbero, G. S. Grest, H. M. Jaeger, G. S. Karczmar, M. E. Möbius, and S. R. Nagel, Phys. Rev. Lett. **96**, 038001 (2006).
  - [8] A. Ries, D. E. Wolf, and T. Unger, Phys. Rev. E **76**, 051301 (2007), arXiv:0704.2392 (cond-mat.soft).
  - [9] M. Depken, J. B. Lechman, M. van Hecke, W. van Saarloos, and G. S. Grest, Europhys. Lett. **78**, 58001 (2007).
  - [10] K. Nichol, A. Zanin, R. Bastien, E. Wandersman, and M. van Hecke, Phys. Rev. Lett. **104**, 078302 (2010).
  - [11] P. Jop, Y. Forterre, and O. Pouliquen, Nature **441**, 727 (2006).
  - [12] P. Jop, Phys. Rev. E **77**, 032301 (2008).
  - [13] M. Jean, Comput. Methods Appl. Mech. Engrg. **177**, 235 (1999).
  - [14] L. Brendel, T. Unger, and D. E. Wolf, in *The Physics of Granular Media* (Wiley-VCH, Weinheim, 2004), pp. 325–343.
  - [15] M. R. Shaebani, T. Unger, and J. Kertesz, International Journal of Modern Physics C **20**, 847867 (2009).
  - [16] J. J. Moreau, Eur. J. Mech. A-Solids **13**, 93 (1994).
  - [17] H. C. Andersen, J. Chem. Phys. **72**, 2384 (1980).
  - [18] T. Börzsönyi, T. Unger, and B. Szabó, Phys. Rev. E **80**, 060302 (2009).
  - [19] H. A. Knudsen and J. Bergli, PRL **103**, 108301 (2009).
  - [20] The sizes  $L_x$ ,  $L_y$  and  $L_z$  were varied one by one in the range from 10 to 60 and the total number of grains were changed accordingly. These tests left the solid fraction and the stress tensor unchanged.